Journal of Multidisciplinary Engineering Science and Technology (JMEST)
ISSN: 3159-0040
Vol. 1 Issue 5, December - 2014

Experimental Wake Studies of a Mining Truck

W.R. Sexton, C.P. Britcher, A.O. Demuren
Dept. of Mechanical & Aerospace Engineering, Old Dominion University
Norfolk, Virginia, USA

***Abstract*—Modern mining operations are highly reliant on the amount of material that can be removed from the earth, and transported to processing plants. Companies that design and build mining dump trucks concentrate on improving the material payload capacity and reliability. Since these trucks operate mainly in off-road conditions, dust dispersion is a major problem. As a result of asymmetry and shear size, complex turbulent flow is created around, and behind these trucks during operation. Wind-tunnel measurements of the wake behind a 1:30-scaled, 400 ton-class mining truck are made with Particle Image Velocimetry. A Proper Orthogonal Decomposition post-process analysis is used to identify most energetic turbulent structures in the wake. These can be used to predict dust dispersion.**

Keywords—turbulent wakes, mining truck, proper orthogonal decomposition

I. Introduction

Vehicle wake can be complex due to size and shape of the vehicle. In most instances, wind-tunnel measurements of simple bodied vehicles lead to insight on aerodynamic characteristics and possible improvements in reducing drag. To the mining industry, a major concern with mining trucks is dust emission that poses health and safety issues for the mining companies and its personnel. Productivity is affected by reduced visibility and increased maintenance needs for mining equipment due to dust fouling. The wake, or low-pressure zone, behind the trucks is the area that dust particles, which are picked-up and released from the huge tires, are entrained and suspended in air. Reed and Organiscak [1] reported that more than 75% of the total dust emissions of a mine could be attributed to the mining trucks driving over the unpaved roads.

To examine the wake, wind-tunnel measurements of the flow around a 1:30-scaled, 400ton-class mining truck are made with a two-dimensional (2-d) Particle Image Velocimetry (PIV) technique. Three key planes are investigated, namely behind each set of rear double tires and at the center-plane of the truck. Streamlines and velocity profiles show the effect of asymmetry from one side to the other and the effect of the high ground clearance of the truck. The wind-tunnel study, discussed in this paper, is part of a larger study to validate CFD simulations reported more fully in Sexton [2].

II. Previous Studies

Research on the wake behind mining trucks is limited. As such, the wind-tunnel measurements of a simplified car body and heavy truck (tractor-trailer) bodies are examined. Lienhart and Becker [3] performed a comprehensive study using Laser Doppler Anemometry, Hot-Wire Anemometry and static pressure measurements, in order to investigate the flow and turbulence structure around a simplified car model, known as the Ahmed model (Ahmed et al. [4]). They collected measurements at 40 m/s (bulk velocity) with two different rear body slant angles (25^o and 35^o), which bracket the critical angle of 30^o, where separated wake flow occurs. They noted that laser optical techniques are able to provide reliable measurements in high turbulence flow fields including flow reversals. They observed that, for both car bodies, in the near wake region some periodic content in the velocity signal could be identified as evidence of vortex shedding.

McCallen et al. [5] reported experimental studies with 1:14 scaled tractor-trailer models at Reynolds numbers between of $0.5x10^6$ and $2.0x10^6$. Techniques such as 3-dimensional Particle Image Velocimetry (3-dPIV), oil-film interferometry, pressure sensitive paint, and hot-film sensors were used. Using 3-dPIV, they measured velocity components in the wake and discovered a 20% reduction in drag with boat-tail plates over the baseline without the plates. They noted that a full-scale test showed only 10% reduction.

Wei et al. [6] conducted CFD simulations of a mining truck and found a drag coefficient of 0.9184 and reported that was within 5% of experimental results. With aerodynamic modifications to the truck the best drag coefficient they achieved was 0.7926. This shows the poor aerodynamics of a mining truck and the difficulty to improve it because of the functional based design.

These demonstrate experimental difficulties associated with truck model studies. All the experiments were performed to collect data for validations of CFD simulations.

III. Experiments

A. Experimental Setup

The Aerolab Inc manufactured wind-tunnel is a fan-driven, closed-return system operated at atmospheric pressure. The dimensions of the test section were 8ft long, 4ft wide, and 3ft high (2.44m x 1.22m x 0.91m). The operating range is 10m/s to 55m/s. The turbulent intensity level was rated at ≥0.2%.

Figure 1 shows a schematic of the experimental setup. Micro-sized particles were introduced with an Antari Z1500 Pro fogger placed upstream of the fan. The PIV system has four components – the synchronizer, the laser, camera(s), and a computer fitted with a "frame grabber" card. The synchronizer controls the timing between the laser pulse and the camera images. To create one laser sheet, two lasers in parallel designed in a single unit are used. Within the single laser unit there are dual Nd:Yag lasers rated at 2-400mJ of energy with a pulse rate of 5-10ns. The laser of the PIV system was placed on top of the tunnel test section and oriented such that the laser sheet was parallel to the flow. With a 1024x1024 CCD camera positioned on the side of the tunnel perpendicular to the laser sheet, the desktop PC outfitted with a "frame grabber" card records the correlation images, generates the interrogation regions, calculates the particle spatial correlation and velocities, and ultimately outputs a single image with a field of velocity vectors. It has been shown that, by overlaying a pair of correlated images, a double exposed image is obtained. This image is divided into small interrogation regions where spatial correlation relates the velocity of particles between the paired correlation images ($\Delta x/\Delta t$). He reported that the accuracy of the PIV velocity calculation is on the order of 10^{-3} when the velocity is on the order of 100m/s.

B. Model Setup

The general design, which is modeled after the CAT797 truck, is asymmetric due to the right side location of the driver's cabin, the design of the cab superstructure, and the different sized hydraulic tanks mounted to the outside of the chassis rails. The truck was 1:30 scaled model. It measured (L=) 0.484m long, 0.275m tall and 0.325m wide. The model was mounted to a 6ft long by 2ft wide (1.83m x 0.61m), 5/8" thick wooden platform. The leading edge of the platform was rounded over. The truck was positioned ~3/4-truck lengths from the leading edge of the platform leaving ~2-truck lengths behind. The platform was mounted so that the leading edge was about 2ft (0.61m, ~1.3 truck lengths) from the entrance to the test section. Centered spanwise on the platform there were ~0.4-truck widths from either side of the platform and ~1.3-truck widths to the walls of the tunnel. The platform was elevated about 6in (0.15m) above the test section floor which left ~1.7-truck heights to the ceiling.

C. Experimental Procedure

Measurements were made in three streamwise vertical planes behind the truck; namely ‘driver plane’, ‘mid plane’, and ‘passenger plane’. Each plane had dimensions X/L = 1.22 by Y/L = 0.92 (23 inches by 17.5 inches). For each plane the laser was repositioned for three streamwise locations.

Repositioning the laser sheet was necessary because the exposure area of the camera was about 4x5in with a 35mm lens. To cover the entirety of the plane, the camera was elevated to three road (platform)-normal placements at each streamwise laser sheet position. Therefore, a series of nine frames were taken for each of the three planes. Because of the shadow of the trailing end of the dump-bed, a vertical electronic mask in the PIV software was added from the road surface to the dump-bed to prevent poor particle correlations. Paired correlation images were set at an interval of dt = 50ms. The pulse rate was set 3.75Hz; this was the fastest rate at which the laser, synchronizer, and computer could capture and record the paired images. The velocity in the test section of the wind-tunnel was set to 14m/s ±0.2m/s. When the wind-tunnel velocity was stable, fog was introduced in order to seed the air, and sample vector fields were recorded. Adjustments in the camera position and focus and fog density were made at this point until a complete vector field was obtained. With a satisfactory setup, 200 paired correlation images were taken at the given frame. At the completion of one frame, the procedure was repeated for the other frames. After all the paired images for each of the 27 frames (9 frames per plane, for each of the 3 planes) were collected, 200 complete vector fields were available for each frame, which are utilized for further processing. It was necessary to adjust the coordinates within each frame to correspond to its respective location within the plane. The coordinate offset was determined by matching the mean velocity fields in the boundaries of the individual frames. The coordinates of each of the 200 vector fields were corrected, as needed, and all nine frames were combined together to comprise 200 vector fields of each plane. Statistics of the velocity profiles and streamlines were developed from these vector fields.

IV. Results

Figures 2 (a) – (f) show measured profiles of the mean streamwise and vertical velocity components *U* and *V* and Fig. 3 shows the corresponding streamlines. Small variation in the profiles near Y/L = 0.3 and 0.6 were results of overlapping uncertainties in the frames during reconstruction of the planes. Above Y/L = 0.6 is the freestream region above the truck. Between Y/L = 0.4 and 0.6 is the sloping end of the dump bed, and below Y/L = 0.4 is the area directly behind the chassis and tires. There is a strong three-dimensional vortex in this wake region, which is a main focus of this study. (Values were non-dimensionalized by truck length, L = 0.484m and velocity, Uref = 14m/s).

In the driver plane in Fig 2, *U* profiles show a negative streamwise velocity region that extends to at least X/L = 0.4 and as high as Y/L = 0.15. In the road-normal, *V*, profile a transition occurs between Y/L = 0.3 and 0.55 from a downward velocity from above the dump bed to a zero normal velocity region below the bed is seen at nearly every downstream location. Flow streamlines constructed from these velocity profiles are shown in Fig. 3. The streamlines for the driver plane, Fig. 3 (a), show a vortex centered at X/L = 0.5 and Y/L = 0.075, near the road surface and behind the truck. The streamwise, *U*, profiles for the mid plane

(centerline, facing front of the truck) shows a gradual decrease in velocity from the freestream to the road surface, with a small reverse flow region at the road surface at X/L = 0.4. The mid plane road-normal profiles are more dramatic due to the air accelerated under the chassis and escaping into the wake region. The mid plane streamlines show a distinct recirculation vortex centered at X/L = 0.3 and Y/L = 0.1. The velocity profiles for the passenger plane (left side, facing front of the truck) show similarities to the profiles of the driver plane.

The difference lies in the location of the recirculation vortex in the streamlines. The passenger plane streamlines show the recirculation vortex located centered near X/L = 0.05 and Y/L = 0.15. Flow visualization shows that this primary vortex is unsteady, being periodically swept away by the accelerating fluid under the truck chassis and between the wheels.

Reynolds Stresses $\langle u^2 \rangle$, $\langle v^2 \rangle$, and $\langle uv \rangle$, computed from the PIV correlations of velocity fields are presented in Fig. 4, for the mid plane. These Reynolds Stress profiles show that the wake behind the truck, between Y/L = 0.1 and 0.5, is highly turbulent and the effect extends way beyond one truck length. Therefore it is easy to understand why, in practice, dust particles which are "kicked-up" by the tires and swept into the wake would have sufficient turbulence energy to remain in suspension for long distances behind the truck. This is one of the major operational problems for mining trucks in the field.

A. Reduced Order Modeling

Also known as low-dimensional modeling, reduced order modeling provides a significant reduction in degrees of freedom while retaining vital system information. A way to determine the vital system information for a practical approximation of a turbulent flow is to separate the turbulent structures by their respective energies and capture only those that constitute the majority of the total kinetic energy.

Turbulent structures with the most energy have the largest length scales, while the smallest structures, which are more numerous, contain lower energies. A mathematical technique called Proper Orthogonal Decomposition (POD) was used to separate and order the turbulent flow structures in the measured planes.

Reichert et al. [7] showed how POD could be applied to turbulent flows. They explained that the three principal components of the POD mathematical procedure are - the two-point velocity correlation tensor R_{ij}, the integral eigensystem equation, and random modal coefficients a^m. The two-point correlation tensor is defined as:

$$R_{ij}(X, X') = \langle u(X) u^*(X') \rangle \equiv \overline{u_i(X) u_j(X')} \quad (1)$$

where, *X* and *X'* are different points in the domain. The integral eigensystem equation is:

$$\int_{\Omega} R_{ij}(X, X') \Phi_{j,m}(X') dX' = \lambda^m \Phi_{i,m}(X) \quad (2)$$

In the POD method, an eigensystem mathematically represents the energies by the eigenvalues, I^m, and corresponding modes (or turbulent coherent structures) by the eigenvectors, Fi,m; where "i" is the node number (in the domain) and “m” is the mode number (highest energy modes correspond to m = 1). The random modal coefficients are obtained from the integral, in which the Einstein summation rule, *i=1:3* is utilized:

$$a^m = \int u_i(X) \Phi_{i,m}(X) dX \quad (3)$$

The eigensystem equation is in the form:

$$AF_{j,m} = I^m F_{i,m} \quad (4)$$

where, **A** is the square matrix derived from the two-point velocity correlation tensor that contains flow characteristic information about each point in the domain. A numerical method to solve the eigensystem problem uses a diagonal matrix, **D**, which contains quadrature weights that are products of Δd (incremental distances, i.e., Δx, Δy, or Δz) and trapezoidal-rule integration weights, 0.5,1,1,…,1,1,0.5 for n locations (Ramsay and Silverman, [8]). One simplification (4) reduces to:

$$RD\Phi = \lambda\Phi \quad (5)$$

where **R** is a square matrix. This is the form of the equation that is solved numerically. The mathematical software MATLAB is utilized for the solution. Once the solution is completed, any flow property that is a function of the velocity, such as, the fluctuating velocity components, Reynolds stresses or kinetic energy, can be reconstructed from the three POD components, a^m, I^m, $F_{i,m}$. Some properties, which are indicative of the validity of the POD analysis are summarized in Table 1.

	PIV		
	Driver	Mid	Pass
RΦ - Φλ (Matrix max value)	$2.45\text{x}10^{-17}$	$1.98\text{x}10^{-17}$	$1.93\text{x}10^{-17}$
(inv(Φ))D(Φ)=I (orthonormality)	1	1	1
$E_{tot}(\sum\int\int R_{ii})$	1.50	0.92	1.03
$E_{tot}(\sum\lambda)$	1.25	0.76	0.82
% of E_{tot} of $\sum\lambda$ (1^{st} 100 modes)	83%	83%	80%

Table 1. Testing validity POD matrices’

Based on the grid applied to the experimental planes a total of 41140 modes (POD structures/energies) could be captured. However, since the majority of the system energy is captured in the lowest modes, only the first 100 modes were calculated. Row 1 shows the balance error in the eigensystem equation. Row 2 is a test of orthonormality. Row 3 gives the total energy in the

system and row 4 is the energy captured by the first 100 POD modes. The ratio to the total energy is shown in the last row. Thus, more than 80% of the energy is contained in the first 100 modes. This is a testament of the complexity of the turbulent structure. In comparison, for flow behind circular cylinder [2], 80% of the energy is contained within the first 3 modes. Figure 5 shows, for three planes, the modal energy (l) spectra of the first 100 modes and how the energy decays with increasing mode number. Figure 6 shows the normalized streamwise modal shapes (turbulent structures) for modes m = 1, 30, and 100. The most energetic mode lies between X/L = 0.4 to 0.8 and Y/L = 0 to 0.2, and this corresponds to the primary vortex structure, previously observed; though there is a slight downstream shift in comparison to the mean streamlines shown in Fig 3(b). It is observed that the sizes of the turbulent structures decrease with mode number.

V. Concluding Remarks

2dPIV was used successfully to collect instantaneous and mean velocities measurements in the wake behind a mining truck. The profiles show similarities between the two sides but the streamlines indicate the affects of the asymmetry. The profiles and streamlines on the centerline of the truck show the affect of air accelerated in high ground clearance. The POD analysis successfully separated the turbulent structures and energies of the wake flow in the three planes of the wind-tunnel experiment. Hence, there is a potential to use this method to isolate the main turbulent structures in the wake of the truck, which can then be used subsequently for reconstruction of the vortex structure in the wake. These structures can also be compared to those obtained from numerical simulation.

References

[1] W.R. Reed, and J.A. Organiscak, "Evaluation of dust exposure to truck drivers following the lead haul truck." *SME Annual Meeting*, 28 February – 2 March, pp. 1-9, Salt Lake City, Utah, 2005.

[2] W.R. Sexton, "Turbulent flow studies of a scaled model of a large mining truck - computation and experiments." PhD Dissertation, Old Dominion University, Norfolk, VA, May 2010.

[3] H. Lienhart, and S. Becker, "Flow and turbulent structure in the wake of a simplified car model." *SAE Technical Paper Series*. SAE 2003-01-0656, 2003.

[4] S.R. Ahmed, G. Ramm, and G. Faltin, "Some salient features of the time-averaged ground vehicle wake." *SAE Technical Paper Series*. SAE 840300, 1984.

[5] R. McCallen, D. Flowers, T. Dunn, J. Owens, F. Browand, M. Hammache, A. Leonard, M. Brady, K. Salari, W. Rutledge, J. Ross, B. Storms, J.T. Heineck, D. Driver, J. Bell, S. Walker, and G. Zilliac, "Aerodynamic drag of heavy vehicles (Class7-8): Simulations and benchmarking." *Government/Industry Meeting*, 19-21 June, SAE 2000-01-2209, pp. 1-19, Washington, D.C, 2000.

[6] X. Wei, G. Wang, and S. Feng, "Aerodynamic characteristics about nining dump truck and the improvements of head shape." *Journal of Hydrodynamics* 20(6): 713-718, 2008.

[7] R.S. Reichert, F.F. Hatay, S. Biringen, and A. Huser, "Proper orthogonal decomposition applied to turbulent flow in a square-duct." *Physics of Fluids* 6(9), 1994.

[8] J.O. Ramsay, and B.W. Silverman, eds. *Functional data analysis*. New York: Springer, 1997.

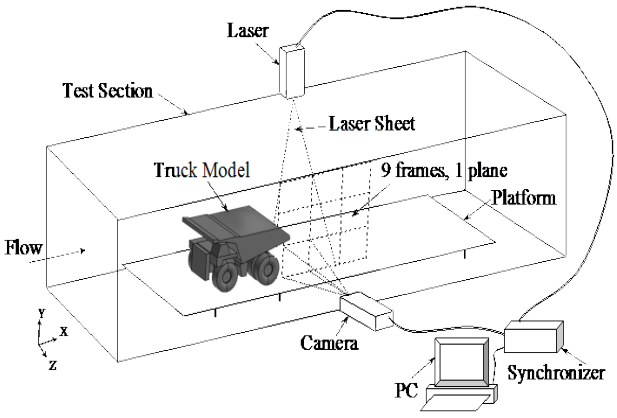

Fig.1. Schematic of the experimental setup (not to scale)

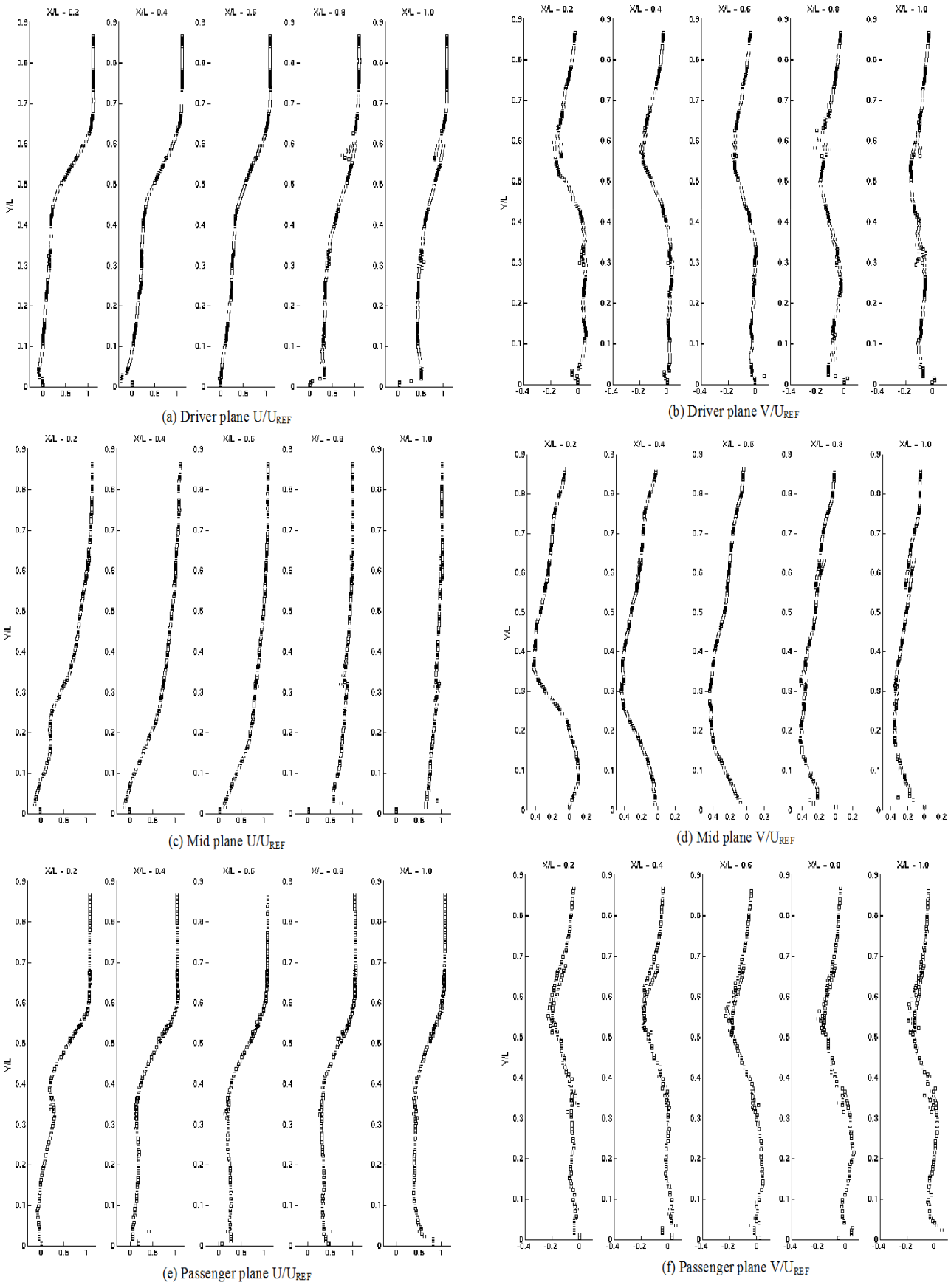

Fig.2.Measured streamwise velocity, U, profiles and road-normal velocity, V, profiles -- driver, mid, and passenger planes

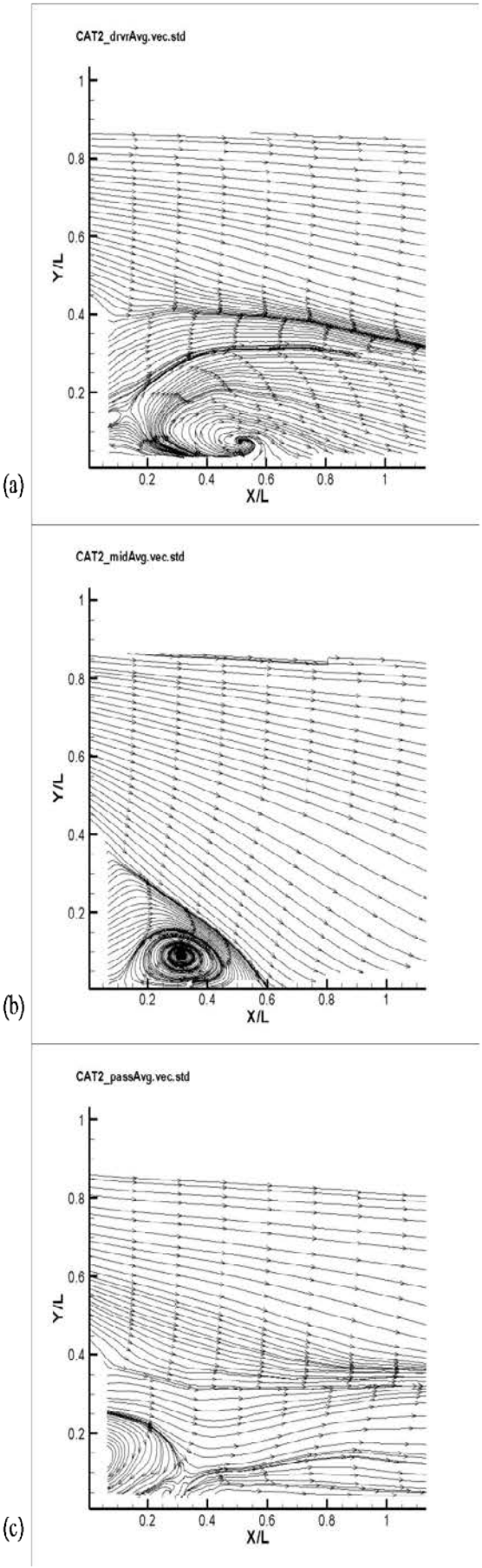

Fig.3. Measured flow streamlines in (a) driver plane, (b) mid plane and (c) passenger plane behind the truck.

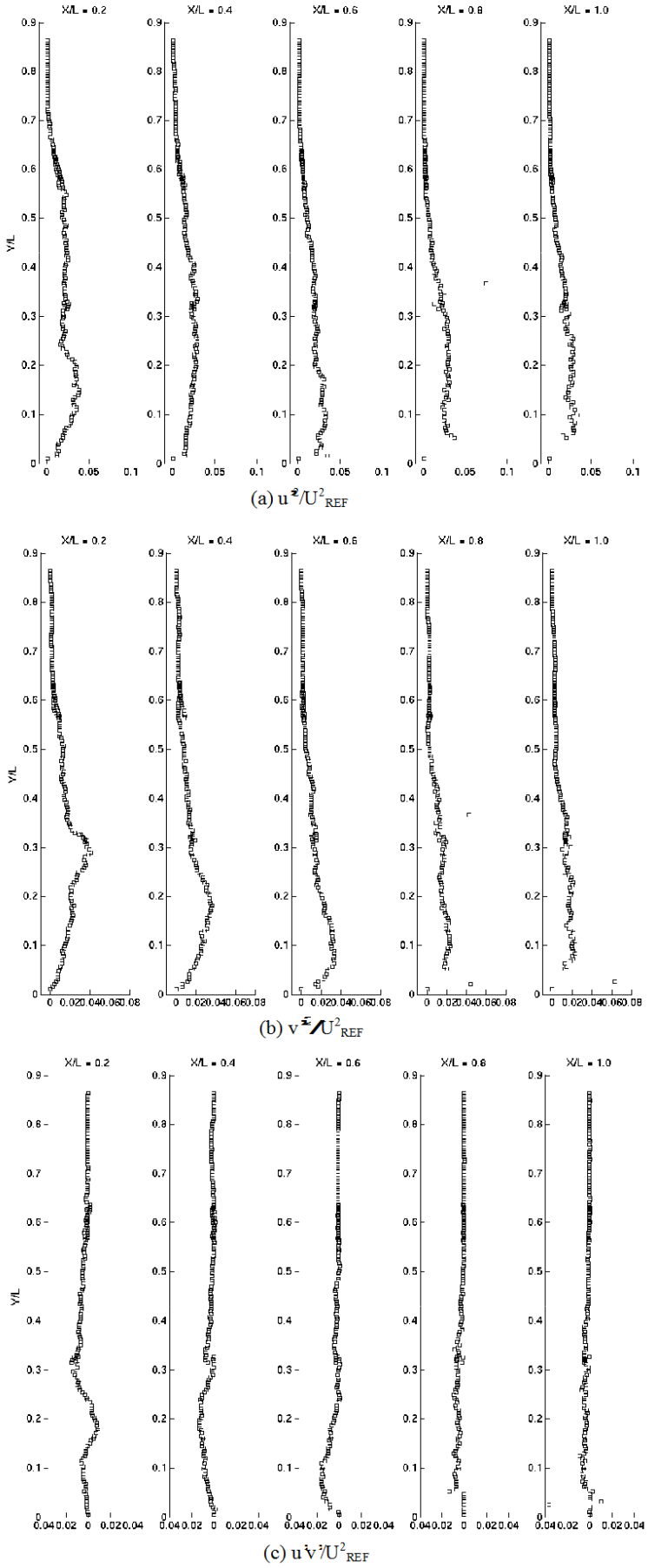

Fig.4. PIV Reynolds stresses in the mid-plane.

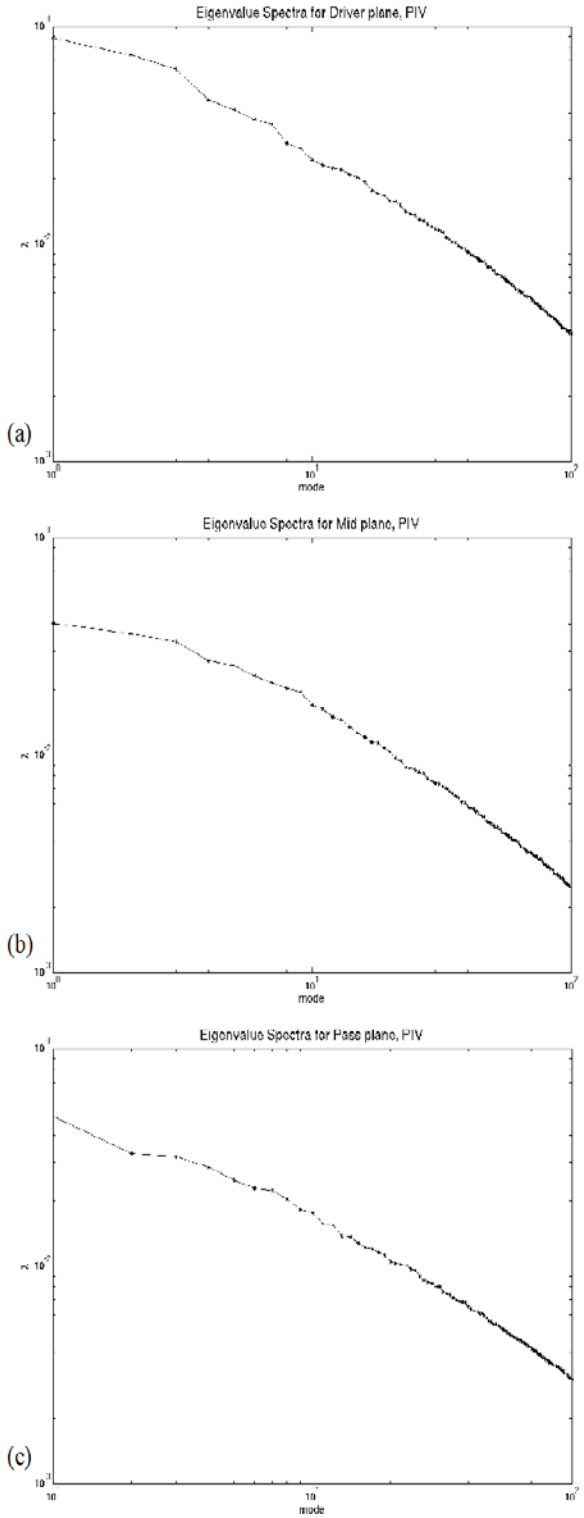

Fig.5. POD modal energy spectra in (a) driver plane, (b) mid plane, and (c) passenger plane behind the truck.

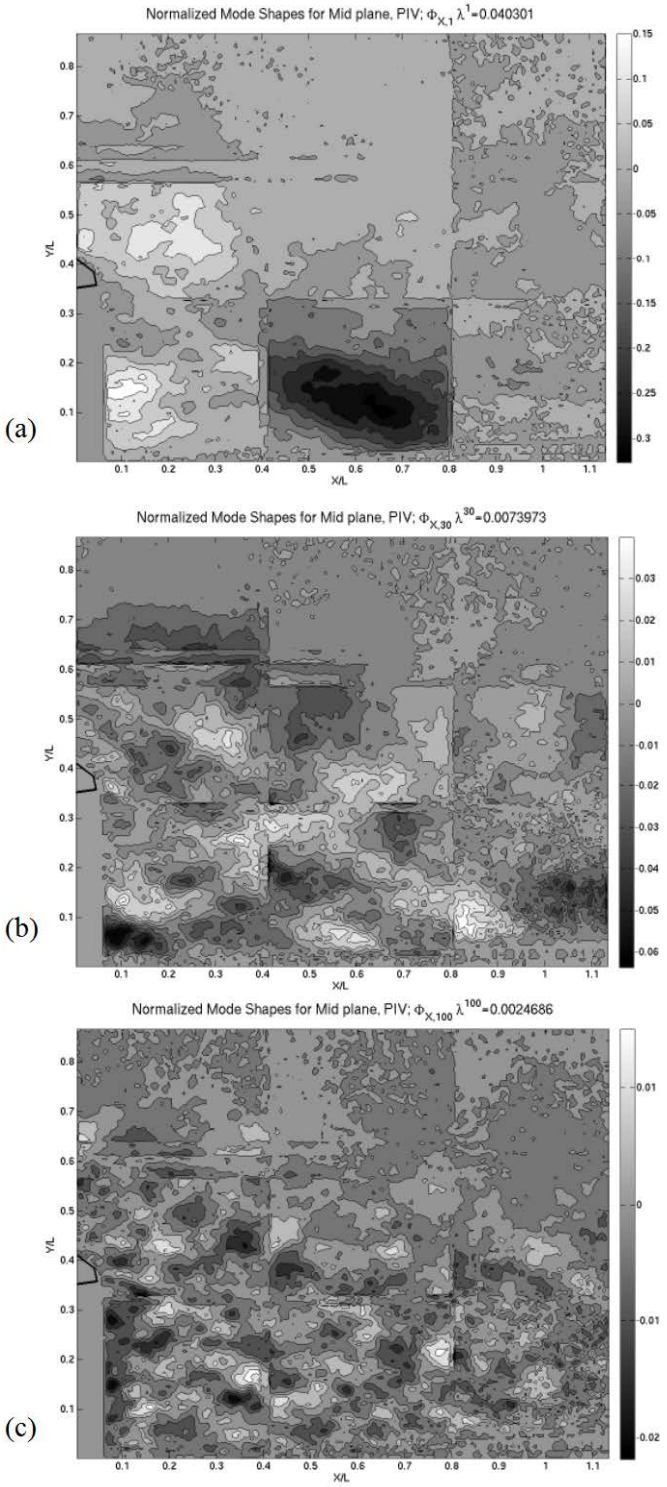

Fig.6. POD normalized streamwise modal shapes at mid-plane for (a) 1, (b) 30, (c) 100; modes.